Stability of a Linear Array of Quasi-2D Vortices

Tsutsui, Nobuyoshi
Department of Earth System Science and Technology, Interdisciplinary Graduate School of Engineering Sciences, Kyushu University

Honji, Hiroyuki
Department of Earth System Science and Technology, Interdisciplinary Graduate School of Engineering Sciences, Kyushu University

https://doi.org/10.15017/16649

出版情報：九州大学大学院総合理工学報告. 23 (4), pp.339-344, 2002-03. Interdisciplinary Graduate School of Engineering Sciences, Kyushu University
バージョン：
権利関係：

九州大学大学院総合理工学報告
第23巻 第4号 339-344頁 平成14年3月

Engineering Sciences Reports, Kyushu University
(KYUSHU DAIGAKU SOGORIKOGAKU HOKOKU)
Vol. 23, No. 4 pp. 339-344 MAR. 2002

Stability of a Linear Array of Quasi-2D Vortices

Nobuyoshi TSUTSUI [*1†] and Hiroyuki HONJI [*2]
[†]E-mail of corresponding author: *tsutsui@esst.kyushu-u.ac.jp*

(Received January 31, 2002)

The stability of a linear array of quasi-two-dimensional (2D) vortices has been investigated using the PIV method in a shallow water tank. An externally imposed Lorentz force is used to drive the vortex array; the force is produced by the interaction between a localized static magnetic field and an electrolytic current passing through a thin layer of fluid. The tracer particle method is used for surface flow visualization. The main findings are as follows. The starting vortex array consists of alternately clockwise and counter-clockwise rotating vortices irrespectively of the dimensionless Lorentz force G. Only when G is larger than 150, the starting vortex array is turned with time into an array of cat's-eye vortices corotating in a selected direction of rotation. When G exceeds further 190 the vortex array becomes unstable and a partially turbulent flow begins to develop. A numerical model is also used to explore some of these phenomena.

Key words: *Lorentz force, vortex array, quasi-2D flow, flow visualization, PIV method*

1. Introduction

The stability of two-dimensional (2D) or quasi-2D flow has been investigated extensively. By 'quasi-2D flow' it is meant here that the relevant flow velocity vectors are approximately horizontal because of the shallowness of the flowing fluid. Recently, diverse types of quasi-2D flows have been studied in the context of nonlinear physics related to dynamics of highly dissipative systems, chaos, fractals, and turbulence. The stability of spatially periodic viscous flows has been investigated by Belotserkovskii *et al.* [1], Gotoh and Yamada [2], Thess [3,4], and others, and many aspects of the flows have been clarified. The stability properties concerning the quasi-2D flows are summarized and reviewed by Murakami [5].

The electromagnetically generated plane periodic flow was investigated by Bondarenko *et al.*[6] experimentally and theoretically. Sommeria and Verron [7] reported the results of an experiment on 2D flows of mercury in a closed domain and their quantitative agreement with a 2D numerical model. Chaotic behavior of a linear array of vortices was investigated experimentally by Tabeling *et al.* [8], in which was reported that the increase of the number of vortices leads to a rapid increase of complexity of the flow regimes of transition to chaos. Cardoso *et al.*[9] also investigated the stability of a linear array of vortices and compared the results to a coupled oscillator model. The stability of a linear array of vortices aligned along a rigid straight wall in fluid was investigated experimentally by Honji[10] and numerically by Nakamura[11]. They reported that a change of cellular vortex pattern occurs when the Lorentz force exceeds some critical value.

In this paper, the laboratory results related to the stability of a linear array of vortices generated in a flat shallow water tank are reported. A comparison with some numerical results will also be made. Although the flow affected by a bottom topography and overall rotation has also been explored, the related results will be reported elsewhere (Tsutsui [12]). In the remainder of the paper, the experimental apparatus is described in section 2, and the experimental results are presented with discussion in section 3. The numerical model and results are addressed in section 4. Some concluding remarks are summarized in section 5.

2. Experimental apparatus

The experimental apparatus is shown schematically in Fig. 1. A shallow water tank made with transparent plastic plates was 50 cm long, 30 cm wide, and 3.0 cm deep. Under the bottom floor of the tank, 4, 8, or 16 circular permanent magnets each with the diameter of 2.10 cm were aligned across the tank with alternating magnetic polarities at the top of each magnet. The case of four magnets is illustrated in Fig. 1; their order of arrangement is N-S-N-S from this to the other side. The white arrows indicate the directions of flows over the magnets. These magnets were actually invisible since the bottom floor of the water tank was painted black for photographic reasons. In Fig. 2, the distribution of the magnitude (B) of magnetic flux density (**B**) measured at the level of fluid surface (z=7.0 mm) is plotted against the

*1 Graduate student, Department of Earth System Science and Technology
*2 Department of Earth System Science and Technology

distance (x) away from the axis of a single magnet. The maximum value of B (B_0 = 0.10 T) is chosen as the representative value of the magnitude of **B** when calculating the values of relevant dimensionless parameters. The tank was filled with a 3.0% aqueous solution of salt water up to the depth of 5.0 mm, and it was served as a working fluid in the experiments. Two circular brass rods with the diameter of 3.0 mm were submerged in the fluid at both sides of the tank and served as the electrodes. When a d.c. voltage (<50V) was applied between the electrodes, an electrolytic current with the density (**J**) passed through the salt water and its interaction with **B** due to the underlying magnets produced the Lorentz force **J**×**B**. This force drove the fluid in the direction normal to both **J** and **B** as indicated by the white arrows in Fig. 1. Surface flow patterns were photographed with a 35 mm or ccd camera from above the tank. The flow patterns were analyzed using a PIV system. It should be noted that the use of the present method is usually limited to quasi-2D shallow flows because an effectively strong magnetic field cannot reach very far.

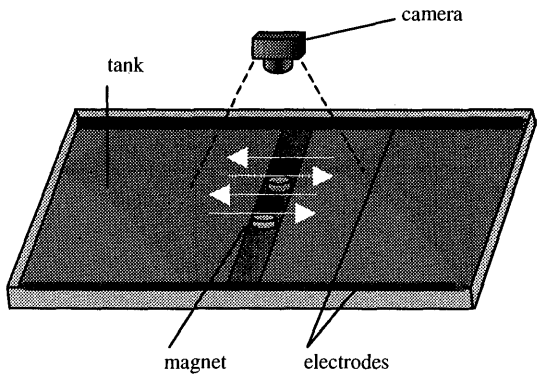

Fig. 1 Experimental setup with four magnets (actually unseen).

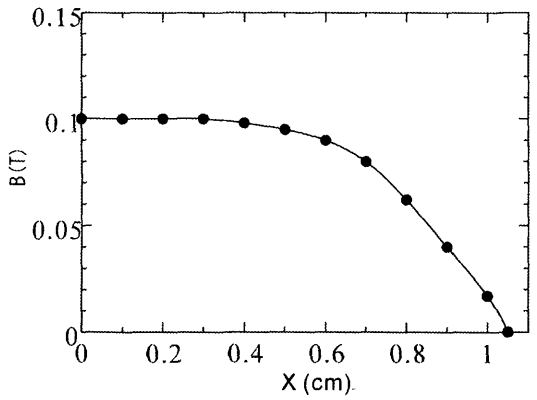

Fig. 2 The distribution of magnetic density (B).

3. Experimental results

The parameters governing the surface flow patterns are the dimensionless Lorentz force $G = (J_0B_0d^3/\rho\nu^2)^{1/2}$ and the dimensionless time $\tau = (J_0B_0/\rho d)^{1/2}t$, where d (=2.10 cm) is the diameter of the underlying magnet, ρ the fluid density, ν its kinematic viscosity, and t the time which has elapsed from the onset of electrolyzation of the fluid, respectively. It may be considered that G plays a role of Reynolds number though no uniform flow is concerned here. The parameter τ is relevant only when starting flow patterns are considered. The experiments were conducted at 90<G<250.

At first typical steady flow patterns above a very long array of underlying magnets are shown for three different values of G in Fig. 3. The number of the magnets is not 4 but 16 in the present case. The direction of electric current is from top to bottom in the figure. All the values of τ for Fig. 3 are larger than 40, at which a steady state of the flow is reached sufficiently. Fig. 3(a) shows a typical vortex flow pattern at a relatively small value of G (=91). The flow consists of 15 equal-sized vortices each of which rotates alternately; the neighboring vortices rotate in the opposite directions. In such cases for small G values are always formed (m-1) vortices in the flow, with m being the number of the magnets.

When G exceeds about 150, the number of steady vortices are reduced by half and eight vortices rotating all in the same counter-clockwise direction are formed as shown in Fig. 3(b); the selection of rotating direction depends on the arrangement of underlying magnets. The value of G=150 may be regarded as a first critical value of G (= G_{c1}) at which the array of oppositely rotating neighboring vortices becomes unstable and is rearranged into that of corotating vortices. When G exceeds about 190 the corotating vortex array begins to be turbulent as shown in Fig. 3(c), in which outlines of some vortices are no longer clear. The value of G=190 may be regarded as a second critical value of G (= G_{c2}). Above this a feature of turbulence is present in the flow.

A starting process of the flow at a value of G (=158) within the range $G_{c1} < G < G_{c2}$ is shown in Fig. 4. As in Fig. 4(a) a linear array of fifteen mutually counter-rotating vortices, each of which has a rather small size, is formed initially. As τ is increased, some of the initial vortices grow in size as shown in Fig. 4(b), while the others are squeezed in between the grown-up vortices. The vortex array at this stage of development consists of eight large vortices and seven thinner squeezed ones. As τ is increased further, only the eight counter-clockwise-rotating vortices grow up further, and the other seven clockwise rotating ones completely disappear as shown in Fig. 4(c). In this way the steady vortex array

consists of the eight vortices, which may also be considered as an array of corotating cat's-eye vortices.

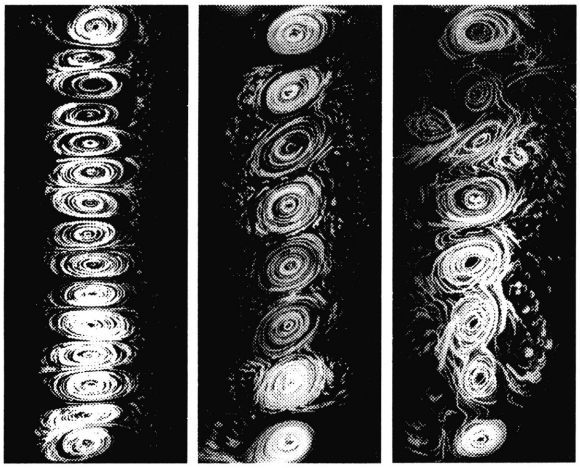

(a) G=91　　(b) G=158　　(c) G=200

Fig. 3 Dependence of steady flow pattern on G at m=16.

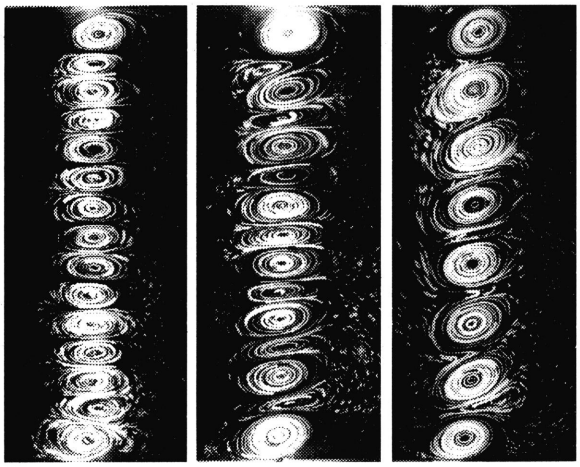

(a) τ = 0.5　　(b) τ = 7.0　　(c) τ = 14.5

Fig. 4 Time development of flow at G=158, m=16.

Until now, the long vortex array only for the case of 16 underlying magnets has been presented. However, the basic features of the vortex array have been found much the same when the even number of the underlying magnets is concerned. Therefore, further investigations have been carried out mainly using 4 or 8 magnets. In these cases the vortex arrays are sufficiently shorter than the tank width, and thus free from the so called end effects due to the existing side walls of the tank. When the odd number of the magnets was used, a resulting vortex array was affected by the arrangement of magnetic polarity of both outermost magnets of the corresponding array. The latter case has been left for further studies.

Figure 5 shows the time development of a vortex array at G=158 in the case of four magnets. Three main mutually counter-rotating vortices are seen to form initially as shown in Fig. 5(a). Outside of the main vortices, additional two vortices are induced weakly in the flow. Our attention, however, will be focused restrictively on the main three vortices. As τ increases, the main part of the flow is still composed of three vortices, a small one being squeezed by outer two large ones, as will be seen from Fig. 5(b). As τ increases further, the squeezed vortex at the center disappears completely, and two counter-clockwise rotating vortices are formed taking the shape of a cat's-eye vortex as shown in Fig. 5(c). As described so far, the basic feature of vortex array formation in the m=4 case does not seem much different from that in the m =16 case.

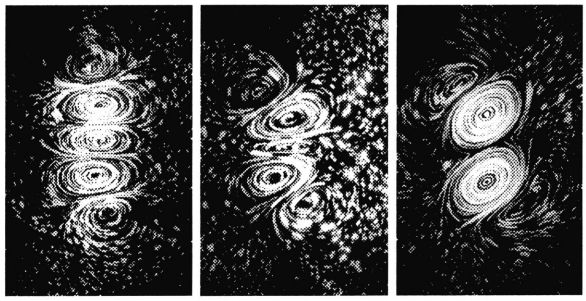

(a) τ = 0.5　　(b) τ = 4.5　　(c) τ = 6.0

Fig. 5 Time development of flow at G=158; m=4.

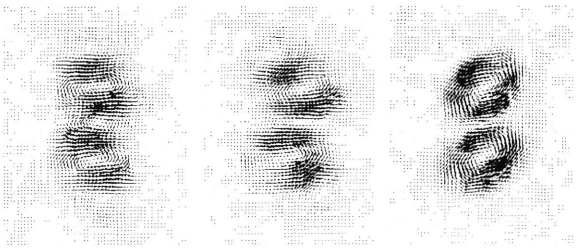

(a) τ = 0.5　　(b) τ = 4.5　　(c) τ = 6.0

Fig. 6 Velocity vector fields at G=158; m=4.

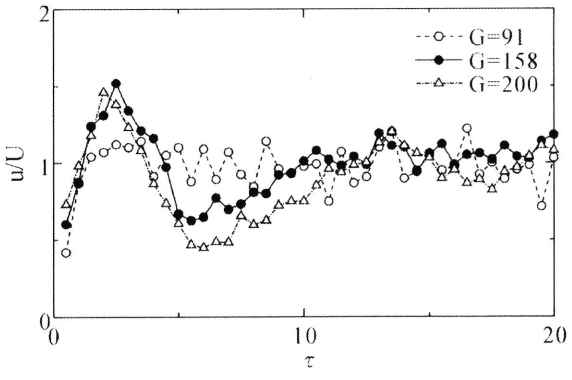

Fig. 7 Time development of u; m=4.

Figure 6 shows the velocity vector fields obtained by means of the PIV analysis of Fig. 5. Again the transition from three to two vortices with time is clear.

Figure 7 shows the time dependence of u, the along-the-tank velocity component at above a magnet center, again obtained by means of the PIV analysis. The representative flow velocity U is here defined as $U = (J_0B_0d/\rho)^{1/2}$. When G = 91 (< G_{c1}) initial velocity changes remain smaller as compared with those in the case of G > G_{c1}. When G is larger than G_{c1} the maximum value of u = 1.5 U is reached at τ = 2, and u becomes approximately equal to U at τ = 10. According to Fig. 6 the steady array of corotating vortices is formed already at τ = 6.0, which is approximately equal to the value of τ where u/U for larger G values begin to increase as will be seen from Fig. 7. The time development of a vortex array in the case of m = 8 is shown in Fig. 8. Immediately after the onset of flow, m-1 (= 7) mutually counter-rotating vortices are formed as shown in Fig. 8(a). As time goes on, some vortices decrease whereas the others increase in size as will be seen from Fig. 8(b). Eventually the flow evolves into a corotating vortex array as shown in Fig. 8(c). The time development of u/U in the case of m = 8 is shown in Fig. 9, in which the general features of curves are similar to the ones in the case of Fig. 7. The maximum value of u = 1.5 U is reached at τ= 3.0 and u becomes approximately equal to U at τ= 10. According to Fig. 8, the corotating vortex array is already completed at = 9.0, where u/U begins to increase as will be seen in Fig. 9. The results so far described concerning Figs. 6 to 9 suggest that as u increases initially an alternating vortex array is formed and, as u begins to decrease after peaking, it becomes unstable. As u begins to increase again after reaching the bottom, the unstable vortex array is rearranged into a steady corotating vortex array with u = U.

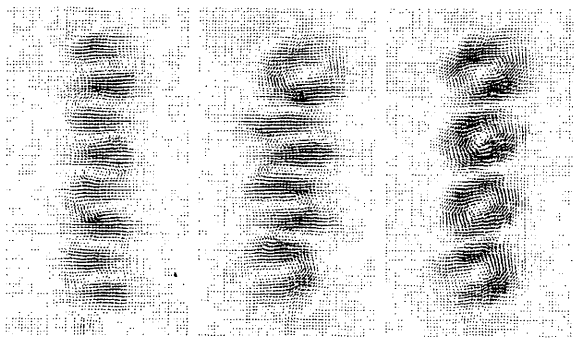

(a) τ = 0.5 (b) τ = 6.0 (c) τ = 9.0

Fig. 8 Velocity vector fields at G=158; m=8.

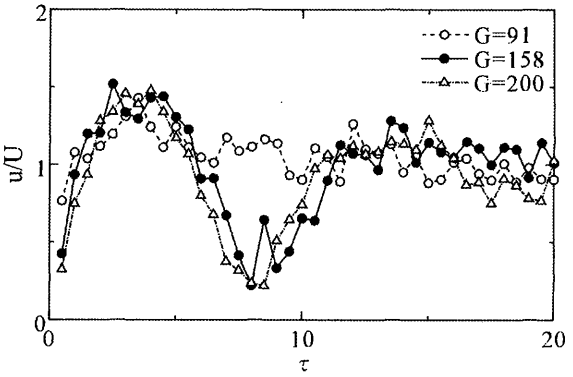

Fig. 9 Time development of u; m= 8.

4. Numerical results

In order to simulate the preceding physical system, the basic equations for quasi-2D flows of a thin layer of fluid driven by the Lorentz force acting only horizontally are considered[5-7]. The equations are,

$$\frac{\partial \mathbf{u}_s}{\partial t} + (\mathbf{u}_s \cdot \nabla_h)\mathbf{u}_s = -\frac{1}{\rho}\nabla_h P - \lambda \mathbf{u}_s + \nu \nabla_h^2 \mathbf{u}_s + \frac{1}{\rho}(\mathbf{J}\times\mathbf{B}) \quad (1)$$

and

$$\nabla_h \cdot \mathbf{u}_s = 0. \quad (2)$$

In Eq. (1) and Eq. (2), $\mathbf{u}_s$ (u,υ) is the surface velocity vector with the along-the-tank x-component u and the transversal y-component υ, p the pressure, ρ the fluid density, h the fluid depth, **J** the electric current density, and **B** the magnetic flux density, respectively. The term **J**×**B** describes the Lorentz force. Letting **i** and **j** be the unit vectors respectively in the x and y directions, we have $\nabla_h = (\partial/\partial x)\mathbf{i}+(\partial/\partial y)\mathbf{j}$. The parameter $\lambda = \chi\,(2\nu/h^2)$ is a friction coefficient due to the existing bottom floor, with χ being a phenomenological parameter that depends on the actual vertical profile of a velocity distribution. The commonly used value of χ in numerical simulations is 1.70 [6]. In the present numerical study, however, we use the value of χ =1.20 for empirical reasons. We assume **J** and **B** as

$$\mathbf{J} = -J_0\mathbf{i} \quad (3)$$

and

$$\mathbf{B} = B_0 \cdot \exp\{\gamma\,(x/d)^2\} \cdot \sin(\pi/d)y \cdot \mathbf{k} \quad (4)$$

respectively, where J_0 is the applied current density, B_0 the maximum value of |**B**| on the axis of a magnet, γ the coefficient connected with the spatial distribution of **B**, and **k** the vertical unit vector. The

Lorentz force **F** is denoted as

$$\mathbf{F} = \mathbf{J}\times\mathbf{B} = -J_0B_0 \cdot \exp\{\gamma (x/d)^2\}\cdot\sin(\pi/d)y \cdot \mathbf{i}. \quad (5)$$

These equations are made dimensionless using $x' = x/d$, $y' = y/d$, and τ substituting Eq. (5) into Eq. (1), taking *rot* of the resulting equation, and introducing the vorticity ω and the streamfunction ψ, we obtain the dimensionless vorticity equation

$$\frac{\partial\omega'}{\partial\tau}+\frac{\partial\psi'}{\partial y'}\frac{\partial\omega'}{\partial x'}-\frac{\partial\psi'}{\partial x'}\frac{\partial\omega'}{\partial y'} = \frac{\nabla_h'^2\omega'}{G}-\frac{\omega'}{R_h}-(\nabla_h'\times\mathbf{F}')_z \quad (6)$$

where the primes indicate non-dimensional quantities, and the dimensionless parameter R_h is defined as

$$R_h = (J_0B_0/\rho d\lambda^2)^{1/2} = G\cdot(h/d)^2\cdot(1/2\chi) \quad (7)$$

and the stream function as

$$\nabla'^2\psi' = -\omega'. \quad (8)$$

The above governing equations are integrated numerically under the boundary conditions $\psi=\omega=0$ at the side walls of the tank.

The simulations are performed with increasing values of the control parameters G and R_h. Figures 10 and 11 show the steady flow patterns developed above the eight aligned magnets. When G is small, a balance between the driving force and the bottom friction gives rise to a linear array of mutually counter-rotating vortices of equal sizes as shown in Fig. 10(a). When G exceeds about 150, four counter clockwise rotating vortices are grown up and three clockwise rotating vortices disappear as shown in Fig. 10(b). Such a vortex array is stable up to G = 190. As G increases further, the flow becomes slightly irregular as shown in Fig. 10(c). The process in the case of Fig. 11 is almost similar to that in the above described case of Fig. 10. These numerical results agree well with the experimentally observed processes described previously in connection with the observed flow patterns and related PIV patterns. The formation of corotating steady vortices is well reproduced at the same critical value of G_{c1}.

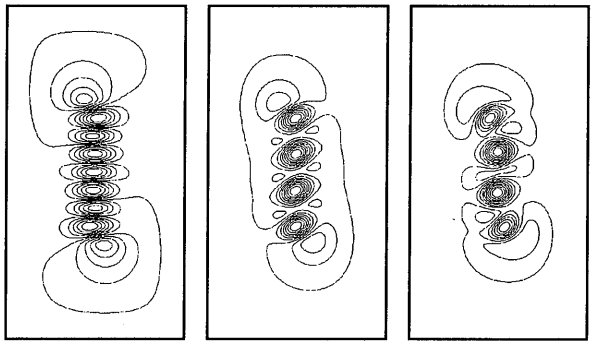

(a) G = 90, R_h = 2.13　(b) G = 160, R_h = 3.78　(c) G = 200, R_h = 4.72

Fig. 10 Computed steady streamline patterns; m = 8.

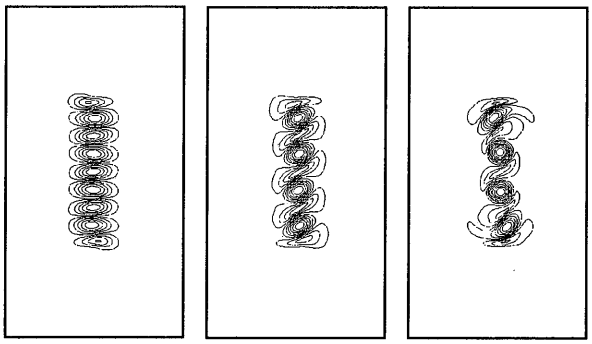

(a) G = 90, R_h = 2.13　(b) G = 160, R_h = 3.78　(c) G = 200, R_h = 4.72

Fig. 11 Computed steady streamline patterns; m = 8.

5. Concluding remarks

The results of experimental and numerical investigations of the stability of quasi-2D vortex arrays formed in a shallow water tank have been described. The PIV method has been used effectively to analyze the time dependent and independent flow patterns. The main findings are as follows. When the dimensionless Lorentz force G is less than 150, the vortex array consists of alternating vortices, of which the neighboring ones rotate in opposite directions. When G is larger than 150, the vortex array becomes unstable and are turned into an array of corotating vortices, of which the number is reduced approximately by half. When G exceeds further 190 outlines of each vortex become unclear and the vortex array is turned to be turbulent. These experimental observations are well reproduced numerically using the quasi-2D model equations with χ being 1.20. No quasi-2D vortex arrays in the case of the odd number of underlying magnets have been studied, though interesting flow patterns slightly different from those described in this paper seem to be formed.

The authors thank Drs. N. Matsunaga, Y. Sugihara, and Y. Ikehata for helpfull discussions.

References

1) S.O. Belotserkovskii, A.P. Mirabel, and M.A. Chusov: On the construction of post-critical mode for a plane periodic flow, Izvestiya, Acad. Sci. USSR, Atomospheric and Oceanic Physics, **14**, 1 (1978) 6 - 12.
2) K. Gotoh and M. Yamada: Instability of cellular flows, J. Phys. Soc. Jpn., **53** (1984) 3395-3398.
3) A. Thess: Instabilities in two-dimensional spatially periodic flows. Pt.I: Kolmogorov flow, Phys. Fluids **A4**, 7 (1992) 1385-1395.
4) A. Thess: Instabilities in two-dimensional spatially periodic flows. Pt.II: Square eddy lattice, Phys. Fluids , **A4**, 7 (1992) 1396-1407.
5) Y. Murakami: Stability of quasi-two-dimensional flows, Nagare, **13** (1994) 115-123.
6) N.F. Bondarenko, M.Z. Gak, and F.V. Dolzhanskiy: Laboratory and theoretical models of plane periodic flows, Izvestiya, Atmospheric and Oceanic Physics, **15**, 10 (1979) 711-716.
7) J. Sommeria and J. Verron: An investigation of nonlinear interactions in a two-dimensional recirculating flow, Phys. Fluids, **27**, 8 (1984) 1918-1920.
8) P. Tabeling, O. Cardoso and B. Perrin : Chaos in a linear array of vortices, J. Fluid. Mech., **213** (1990) 511-530.
9) O. Cardoso, H. Willaime, and P. Tabeling: Short-wavelength instability in a linear array of vortices, Phys. Rev. Lett.,**65**,15 (1990) 1869-1872.
10) H. Honji : Instability of an electromagnetically driven vortex array, Proc. 6th Asian Congr. Fluid Mech.,(1995) 1218-1221.
11) Y. Nakamura: Transition to turbulence from a localized vortex array, J. Phys. Soc. Jpn., **65**, 6 (1996) 1666-1672.
12) N.Tsutsui: Stability of a linear array of quasi-two-dimensional vortices, M. Sci. Thesis, Interdisciplinary Gr. Sch. Eng. Sci., Kyushu Univ., March 2002.